第 29 卷第 12 期 无 机 化 学 学 报 Vol.29 No.12
2013 年 12 月 CHINESE JOURNAL OF INORGANIC CHEMISTRY 2695-2703

金属铂(Ⅱ)-卟啉二聚体配合物的分子内 π-π 相互作用

苏祎伟 骆开均* 张晨阳 郭清 刘汉林 王 燕
(四川师范大学化学与材料科学学院,成都 610068)

摘要:合成了以不同链长的烷氧基柔性链相连接的金属铂(Ⅱ)-卟啉二聚体配合物并对其热稳定性,光谱性质及电化学性质做了研究。在浓度由 10^{-7} mol·dm^{-3} 增大到 10^{-3} mol·dm^{-3} 的过程中将配体与配合物的紫外-可见吸收光谱与光致发光光谱做了对比,发现配体与配合物的吸收光谱随浓度变化未出现改变,但发射光谱显现出随浓度增大而产生红移现象。当烷氧基柔性链中碳原子数大于 4 时,C6 与 C10 配合物无论是高浓度下的溶液与升华固体薄膜中的荧光发射光谱均比配体有明显的红移,而短链的配合物无此性质。

关键词:配位化学;分子内相互作用;荧光光谱;金属铂(Ⅱ)-卟啉二聚体配合物;开放与闭合式构象;金属-金属相互作用
中图分类号:O614.82+6 **文献标识码**:A **文章编号**:1001-4861(2013)12-2695-09
DOI:10.3969/j.issn.1001-4861.2013.00.386

Intramolecular π-π Interactions in Platinum(Ⅱ) Metalloporphyrin Dimer Homologues with Aliphatic Chains of Different Lengths

SU Yi-Wei LUO Kai-Jun* ZHANG Chen-Yang GUO Qing LIU Han-Lin WANG Yan
(*College of Chemistry and Materials Science, Sichuan Normal University, Chengdu* 610068, *China*)

Abstract: The synthesis and thermal stabilities, spectroscopic and electrochemical properties for a series of platinum(Ⅱ) metalloporphyrin dimer complexes with aliphatic chain of different lengths [-O(CH_2)$_n$O-] have been studied. Although dimeric porphyrin ligands and platinum(Ⅱ) complexes display nearly the same absorption spectra in the concentration range from 10^{-7} to 10^{-4} mol·dm^{-3}, these ligands and their complexes show concentration-dependent emission when the length of aliphatic chain is beyond four carbon atoms. At elevated concentration of the ligands and complexes, the emission spectra show obvious red-shifts. For complex Pt_2C_6(OPTPP)$_2$ and Pt_2C_{10}(OPTPP)$_2$, the emission maxima at 652 nm are red-shifted to 676 and 681 nm at concentrations >10^{-4} mol·dm^{-3}. Emission spectra of the sublimate films of complexes also display similar red-shifts: 43 nm for Pt_2C_6(OPTPP)$_2$ and 53 nm for Pt_2C_{10}(OPTPP)$_2$. The concentration-dependent emission indicates that there are intramolecular π-π interactions in porphyrin dimers and platinum(Ⅱ) metalloporphyrins.

Key words: coordination chemistry; intramolecular interactions; luminescence; platinum(Ⅱ) metalloporphyrin dimer complexes; open and folded conformations; metal-metal interactions

0 Introduction

Luminescent square-planar platinum(Ⅱ) complexes have attracted considerable interest over the past decades for their potential application in the development of organometallic-based optoelectronics, such as light-emitting devices[1-8], chemosensors[9-12], and photovoltaic dye-sensitized devices[13-14]. In addition,

收稿日期:2013-04-11。收修改稿日期:2013-07-18。
国家自然科学基金(No.21072141,21172161)资助项目。
*通讯联系人。E-mail:luo-k-j007@163.com

square-planar platinum(Ⅱ) complexes are prone to form rich excimer and aggregate dimer through intermolecular or intramolecular π-π and Pt-Pt interactions, leading to remarkable red shifts relative to the isolated platinum (Ⅱ) complex emission spectra [15-19]. Therefore, the excimer and dimer or the combination of monomer and excimer formed in square-planar platinum (Ⅱ) complexes can offer useful means of fabricating near-infrared (NIR) organic light emitting diodes (OLEDs) and single-dopant phosphorescent white organic light emitting diodes (PhWOLEDs)[1,8,20-22]. For example, the electroluminescent devices using neat film emitters made of terdentate cyclometallated phosphorescent Pt (Ⅱ) complexes PtL^nCl can exhibit exclusive NIR excimer emission peaking at wavelengths between 705 and 720 nm and obtain unusually high external quantum efficiencies from 9.8% to 10.7% photons/electron and a high forward light output exceeding 15 mW·cm^{-1} [2,20]. In this work, a series of platinum (Ⅱ) metalloporphyrin dimer complexes with aliphatic chain of different lengths were synthesized and characterized. When the length of aliphatic chain is beyond four carbon atoms, these ligands and their complexes show red- shifted emission in the concentration range from 10^{-7} to 10^{-4} mol·dm^{-3}.

1 Experimental

1.1 Measurements and Materials

General method: All chemicals used were commercial products and of analytical grade. Tetrahydrofuran (THF) was heated under reflux over sodium/benzophenone and freshly distilled before use. Propionic acid, pyrrole, *N*,*N*-dimethylformamide (DMF) and benzonitrile, acetonitrile were dried over anhydrous $MgSO_4$ for over 24 h and freshly distilled prior to use.

The thermogravimetric analysis (TGA) of the complexes was performed under nitrogen atmosphere at a heating rate of 10 ^{o}Cmin^{-1} with a TA Q500 analyzer. UV-Vis absorption spectra were recorded on a Unico UV-4802s spectrometer. Emission spectra were obtained using a Hitachi F-7000 Fluorescence Spectrometer. ^{1}H, ^{13}C NMR spectra were recorded using a Varian Unity 400 MHz spectrometer in $CDCl_3$ or deuterated dimethyl sulfoxide (DMSO-d_6). Mass spectra were recorded on a Finnigan-LCQDECA spectrometer. The cyclic voltammograms were recorded with a voltammetry analyzer (Model LK2003 from Tianjin Lanlike Instrument Co.) in solution of tetrabutylammonium hexafluorophosphate in acetonitrile (0.1 mol·dm^{-3}) with a scanning rate of 0.1 mV·s^{-1} at room temperature. The measuring cell consisted of vitreous carbon electrode as the working electrode, Ag/Ag^+ electrode as the reference electrode, and platinum wire electrode as the auxiliary electrode. The energy levels were calculated with the ferrocene (FOC) value of −4.8 eV with respect to vacuum level as a calibration reference. After the measurement, two drops of FOC in acetonitrile (3 mmol·dm^{-3}) were added and measured for calibration. Therefore, the HOMO levels of the compounds could be calculated by the equation $E_{HOMO}=-e(E_{onset(ox)}-E_{1/2,FOC})-4.8$ eV, and the LUMO level could be estimated by the equation $E_{LUMO}=E_{HOMO}+1\ 240/\lambda_{edge}$ [25], where the $E_{1/2,FOC}$ stands for the half-wave potential of F_c/F_c^+.

1.2 Synthesis

1.2.1 10,15,20-Triphenyl-5-(4-hydroxyphenyl)-21*H*,23*H*-porphyrin(HOPTPP): 4-hydroxybenzaldehyde (1.46 g, 0.012 mol) and benzaldehyde (3.82 g, 0.036 mol) were added in 300 mL propionic acid in a three-necked-flask. The mixture was refluxed for 0.5 h. Freshly distilled pyrrole (3.22 g, 0.048 mol) was then added dropwise and the mixture was refluxed for 0.5 h. The reaction mixture was evaporated to remove 2/3 of the solvent and 100 mL ethanol was added to the cooled residue. This mixture was filtered after 18 h and the crude solid product was washed into purple using ethanol. This crude product was purified by column chromatography (Al_2O_3; $CHCl_3$). The first fraction was 5,10,15,20-tetraphenylporphyrin. Then the eluent was changed into $CHCl_3/CH_3CH_2OH$ (V:V=8:1) and the next fraction was soon washed down. This fraction was purified by column chromatography (SiO_2; CH_2Cl_2/petroleum ether, 5:1, V/V). The first fraction was the title compound. Recrystallization from CH_2Cl_2/CH_3OH gave 420 mg (4.9%) of light purple crystals.

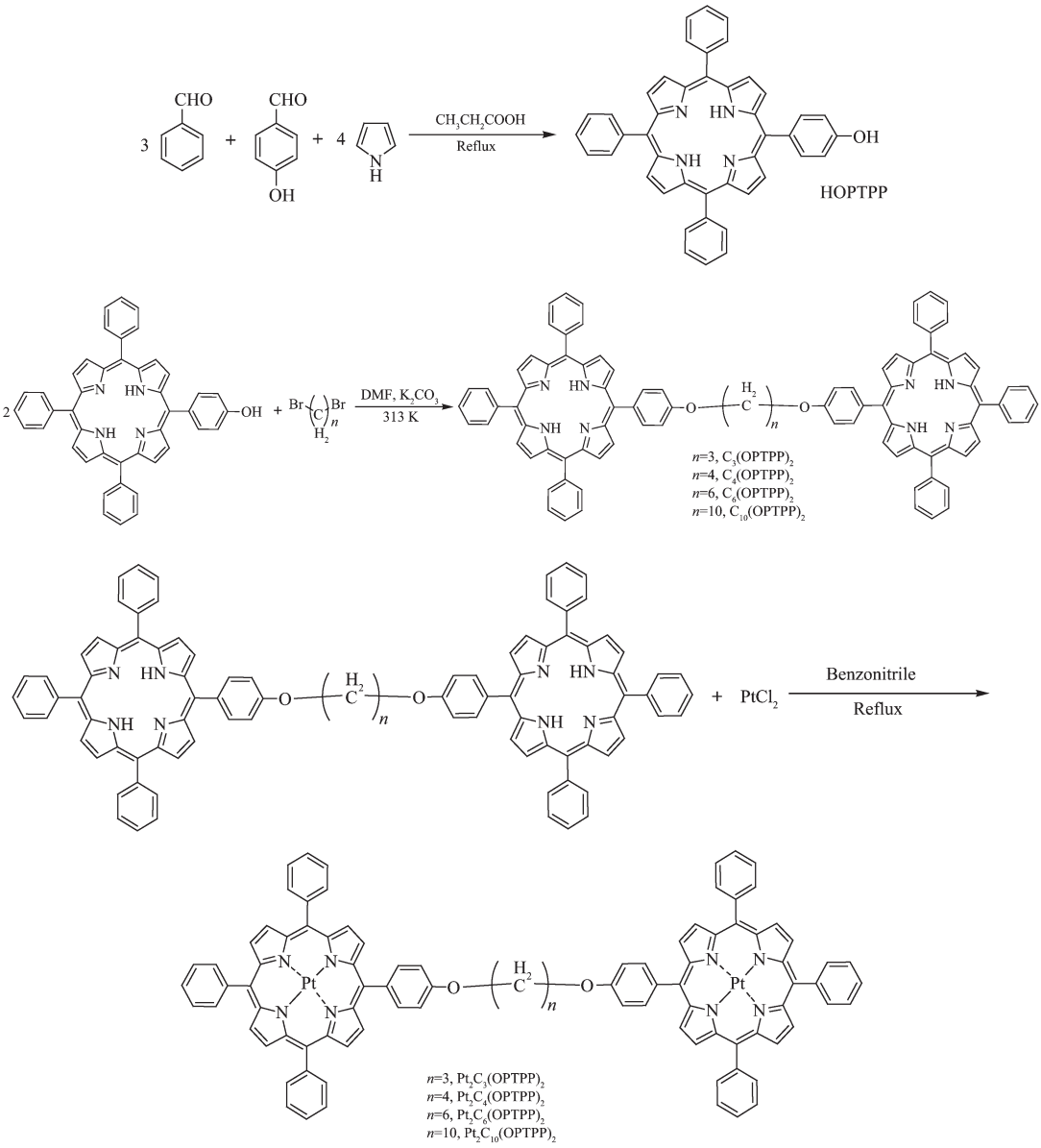

Scheme 1　Synthetic route

^{1}H NMR (400 MHz, DMSO-d_6) δ: 10.010 (s, 1 H, OH), 8.926 (d, 2 H, J=3.6 Hz, β-pyrrolic), 8.824 (d, 2 H, J=3.6 Hz, β-pyrrolic), 8.810 (s, 4 H, β-pyrrolic), 8.232~8.214 (m, 6 H, *o*-phenyl), 8.032 (d, 2 H, J=8.4 Hz, *o*-hydroxyphenyl), 7.840~7.824 (m, 9 H, *o*-, *p*-phenyl), 7.227 (d, 2 H, J=8.4 Hz, *m*-hydroxyphenyl), −2.909 (s, 2 H, inner NH).

1.2.2 Porphyrin dimer with four carbon atoms chain (C_4(OPTPP)$_2$): HOPTPP (120 mg, 0.2 mmol) and K_2CO_3 (0.1 g) were added to DMF (50 mL). 1,4-dibromobutane (32.4 mg, 0.15 mmol) was added dropwise and the mixture was stirred at 40 ℃ for 24 h. Ice water was poured into the reaction flask and the suspension was filtered and washed by water and ethanol. The crude product was purified by column chromatography (SiO_2; $CHCl_3$). The first fraction was further purified by column chromatography (SiO_2; CH_2Cl_2/petroleum ether, 1∶1, *V*/*V*) and the second fraction was the target compound. The product was removed of solvent in vacuo and isolated as dark red powder in 16.4% yield (25 mg). ^{1}H NMR (400 MHz, $CDCl_3$) δ: 8. 920 (d, 4 H, J=4.8 Hz, β-pyrrolic), 8.875 (d, 4 H, J=4.8 Hz, β-pyrrolic), 8.843 (s, 8 H, β-pyrrolic), 8.220~8.197 (m, 12 H, *o*-phenyl), 8.177 (d,

4 H, *J*=7.6 Hz, *o*-hydroxyphenyl), 7.787~7.711 (m, 18 H, *o*-, *p*-phenyl), 7.374 (d, 4 H, *J* =8.4 Hz, *m*-hydroxyphenyl), 4.471 (t, 4 H, *J*=6.4 Hz, α-CH_2), 2.364~2.324 (m, 4 H, β-CH_2), −2.745 (s, 4 H, inner NH). ^{13}C NMR (100 MHz, $CDCl_3$): 27.8 (β-CH_2), 68.7 (α-CH_2), 114.3, 120.1, 127.9, 128.6, 131.0, 135.6, 142.3, 158.6.

The other porphyrin dimers were synthesized using the similar method.

1.2.3 C_3(OPTPP)$_2$ Yield: 18.1%. ^{1}H NMR (400 MHz, $CDCl_3$) δ: 8.930 (d, 4 H, *J*=4.8 Hz, β-pyrrolic), 8.842 (d, 4 H, *J*=4.8 Hz, β-pyrrolic), 8.822 (s, 8 H, β-pyrrolic), 8.234~8.194 (m, 12 H, *o*-phenyl), 8.189~8.176 (d, 4 H, *J*=5.2 Hz, *o*-hydroxyphenyl), 7.784~7.723 (m, 18 H, *o*-, *p*-phenyl), 7.421 (d, 4 H, *J*=8.8 Hz, *m*-hydroxyphenyl), 4.660 (t,4 H, *J*=6.0 Hz, α-CH_2), 2.658 (t, 2 H, *J*=5.6 Hz, β-CH_2), −2.759 (s, 4 H, inner NH). ^{13}C NMR (100 MHz, $CDCl_3$): 29.7 (β-CH_2), 64.8 (α-CH_2), 112.8, 120.0, 126.6, 127.7, 134.5, 135.8, 142.2, 146.6, 158.8.

1.2.4 C_6(OPTPP)$_2$ Yield: 15.4%. ^{1}H NMR (400 MHz, $CDCl_3$) δ: 8.917 (d, 4 H, *J*=4.8 Hz, β-pyrrolic), 8.849 (d, 4 H, *J*=4.8 Hz, β-pyrrolic), 8.820 (s, 8 H, β-pyrrolic), 8.222~8.8.199 (m, 12 H, *o*-phenyl), 8.157 (d, 4 H, *J*=8.4 Hz, *o*-hydroxyphenyl),7.764~7.731 (m, 18H, *o*-, *p*-phenyl), 7.345 (d, 4 H, *J* =8.8 Hz, *m*-hydroxyphenyl), 4.353 (t, 4 H, *J* =6.0 Hz, α-CH_2), 2.173~2.120 (m, 4 H, β-CH_2), 1.857~1.795 (m, 4 H, γ-CH_2), −2.769 (s, 4 H, inner NH). ^{13}C NMR (100 MHz, $CDCl_3$): 25.9 (γ-CH_2), 29.6 (β-CH_2), 68.7 (α-CH_2), 114.3, 120.1, 127.8, 128.9, 131.2, 133.6, 133.9, 142.3, 158.9.

1.2.5 C_{10}(OPTPP)$_2$ Yield: 17.3%. ^{1}H NMR (400 MHz, $CDCl_3$) δ: 8.900 (d, 4 H, *J*=4.4 Hz, β-pyrrolic), 8.848 (d, 4 H, *J*=4.4 Hz, β-pyrrolic), 8.832 (s, 8 H, β-pyrrolic), 8.216~8.198 (m, 12 H, *o*-phenyl), 8.127 (d, 4 H, *J*=8.4 Hz, *o*-hydroxyphenyl), 7.776~7.714 (m, 18 H, *o*-, *p*-phenyl), 7.300 (d, 4 H, *J* =8.8 Hz, *m*-hydroxyphenyl), 4.291 (t, 4 H, J 6.4 Hz, α-CH_2), 2.173~2.095 (m, 4 H, β-CH_2), 1.725~1.662 (m, 4 H, γ-CH_2), 1.317~1.242 (m, 4 H, δ-CH_2), 0.905~0.847 (m, 4 H, ε-CH_2), −2.774 (s, 4 H, inner NH). ^{13}C NMR (100 MHz, $CDCl_3$): 26.1 (γ-, δ-, ε-CH_2), 29.7 (β-CH_2), 68.8 (α-CH_2), 112.7, 120.2, 126.7, 127.7, 131.5, 134.6, 135.6, 142.2, 159.1.

1.2.6 Platinum (Ⅱ) Metalloporphyrin Dimer Complexes with carbon chain (Pt_2C_4(OPTPP)$_2$): $PtCl_2$ (24.4 mg, 0.092 mmol) was added to benzonitrile (11 mL) and the mixture was refluxed for 5 h. Add C_4(OPTPP)$_2$ (35.6 mg, 0.027 mmol) into the flask and keep refluxing for 3 h. After removal of solvent in vacuo, the residue was purified through column chromatography (SiO_2; $CHCl_3$/petroleum ether, 1∶1, *V*/*V*). Collect the orange fraction and after removing the solvent the orange powder was obtained in 16.7% yield (9.87 mg). ^{1}H NMR (400 MHz, $CDCl_3$) δ: 8.944 (d, 4 H, *J*=4.8 Hz, β-pyrrolic), 8.832 (d, 4 H, *J*=4.8 Hz, β-pyrrolic), 8.744 (s, 8 H, β-pyrrolic), 8.219~8.153 (m, 12 H, *o*-phenyl), 8.144 (d, 4 H, *J*=8.0 Hz, *o*-hydroxyphenyl), 7.759~7.694 (m, 18 H, *o*-, *p*-phenyl), 7.339 (d, 4 H, *J*=8.4 Hz, *m*-hydroxyphenyl), 4.441 (t, 4 H, *J*=5.2 Hz, α-CH_2), 2.348 (m, 4 H, β-CH_2). ^{13}C NMR (100 MHz, $CDCl_3$): 27.8 (β-CH_2), 68.7 (α-CH_2), 114.3, 120.6, 127.8, 128.5, 131.6, 135.6, 143.3, 158.6. MS-ESI *m*/*z* 1701.4 $[M+1]^+$.

The other complexes were synthesized in a similar way.

1.2.7 Pt_2C_3(OPTPP)$_2$ Yield: 14.3%. ^{1}H NMR (400 MHz, $CDCl_3$) δ: 8.835 (d, 4 H, *J*=5.2 Hz, β-pyrrolic), 8.748 (d, 4 H, *J*=5.2 Hz, β-pyrrolic), 8.730 (s, 8 H, β-pyrrolic), 8.163~8.140 (m, 12 H, *o*-phenyl), 8.121 (d, 4 H, *J*=8.8 Hz, *o*-hydroxyphenyl), 7.766~7.683 (m, 18 H, *o*-, *p*-phenyl),7.376 (d, 4 H, *J*=8.4 Hz, *m*-hydroxyphenyl), 4.615 (t, 4 H, *J*=5.8 Hz, α-CH_2), 2.655 (t, 2 H, *J*=5.6 Hz, β-CH_2). ^{13}C NMR (100 MHz, $CDCl_3$): 29.5 (β-CH_2), 64.9 (α-CH_2), 113.8, 120.4, 126.4, 127.9, 134.8, 135.8, 142.2, 145.7, 158.8. MS-ESI *m*/*z* 1686.4 $[M+1]^+$.

1.2.8 Pt_2C_6(OPTPP)$_2$ Yield: 15.1%. ^{1}H NMR (400 MHz, $CDCl_3$) δ: 8.827 (d, 4 H, *J*=5.2 Hz, β-pyrrolic), 8.804 (d, 4 H, *J*=4.8 Hz, β-pyrrolic), 8.756 (s, 8 H, β-pyrrolic), 8.153~8.083 (m, 12 H, *o*-phenyl), 8.061 (d, 4 H, J 8.4 Hz, *o*-hydroxyphenyl), 7.765~7.711 (m, 18 H, *o*-, *p*-phenyl), 7.316 (d, 4 H, *J*=8.8 Hz, *m*-hydroxyphenyl), 4.350 (t, 4 H, *J*=6.4 Hz, α-CH_2), 2.338 (m, 4 H, β-CH_2), 2.104 (m, 4 H, γ-CH_2). ^{13}C NMR (100

MHz, $CDCl_3$): 25.9 (γ-CH_2), 29.6 (β-CH_2), 68.7 (α-CH_2), 114.4, 120.1, 127.4, 128.9, 130.7, 133.6, 133.8, 142.3, 158.9. MS-ESI *m/z* 1728.5 $[M+1]^+$.

1.2.9 $Pt_2C_{10}(OPTPP)_2$ Yield: 15.4%. ^1H NMR (400 MHz, $CDCl_3$) δ: 8.809 (d, 4 H, *J*=4.8 Hz, β-pyrrolic), 8.796 (d, 4 H, *J*=5.2 Hz, β-pyrrolic), 8.734 (s, 8 H, β-pyrrolic), 8.144~8.130 (m, 12 H, *o*-phenyl), 8.049 (d, 4 H, *J*=8 Hz, *o*-hydroxyphenyl), 7.741~7.706 (m, 18 H, *o*-, *p*-phenyl), 7.308 (d, 4 H, *J*=8.4 Hz, *m*-hydroxyphenyl), 4.256 (t, 4 H, J 4.8 Hz, α-CH_2), 2.009~1.936 (m, 4 H, β-CH_2), 1.551 ~1.512 (m, 4 H, γ-CH_2), 1.333~1.284 (m, 4 H, δ-CH_2), 0.954~0.880 (m, 4 H, ε-CH_2). ^{13}C NMR (100 MHz, $CDCl_3$): 26.1 (γ-, δ-, ε-CH_2), 29.6 (β-CH_2), 69.0 (α-CH_2), 112.7, 120.5, 126.9, 127.7, 131.4, 134.6, 135.8, 142.3, 159.1. MS-ESI *m/z* 1784.5 $[M+1]^+$.

2 Results and discussion

2.1 UV-Vis absorption spectra

The UV-Vis absorption data of the ligands and complexes are summarized in Table 1. Because of analogous molecular structure of the complexes we take binuclear porphyrin ligand $C_6(OPTPP)_2$ and its complex as an example to discuss the UV-Vis absorption. The electronic spectra of the porphyrin ligand and its complex are shown in Fig.1. The absorption spectra of the ligand display strong transition for the Soret band (B band) near 426 nm. The Q band is located at 514 nm, 548 nm, 591 nm, 648 nm, respectively. With the formation of the platinum(Ⅱ) complexe the Soret band is blue-shifted from the absorption of the ligands. The peaks of Q band are decreased by two and are blue-shifted to 509 nm and 539 nm. This change reveals the formation of the Pt(Ⅱ)-porphyrin complexes because when the 4 N atoms are coordinated with Pt(Ⅱ) the symmetry of the porphyrin molecule is improved and thus making the energy levels closer to each other. For the interaction between e_g ($d\pi$) of the metal ion and e_g (LUMO) of porphyrin ligand, the energy level of LUMO rises, which leads to the blue-shift of the Soret and Q band.

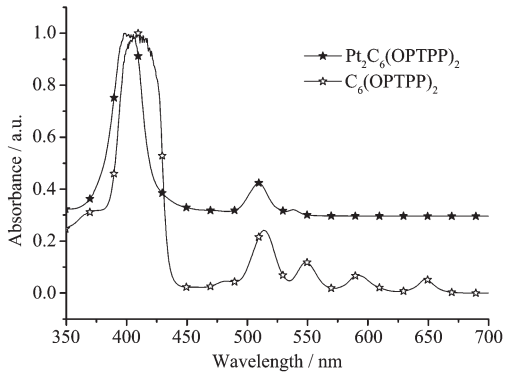

Fig.1 UV-Vis absorption spectra of ligand $C_6(OPTPP)_2$ and complex $Pt_2C_6(OPTPP)_2$ in THF solution

2.2 Emission spectra

The concentration-dependent emission data of porphyrin dimer ligands in tetrahydrofuran (THF) are listed in Table 2. Fig.2 (a) is emission spectra of ligand $C_6(OPTPP)_2$ in the concentration range from 10^{-3} to 10^{-7} mol·dm^{-3}. With the increment of concentration of porphyrin dimer ligand, the emission maxima in THF at 298 K are red-shifted on an average of 22 nm and the intensity of the emission

Table 1 Absorption data of porphyrin ligands and platinum(Ⅱ) complexes in THF solution at 298 K, concentration: 10 μmol·dm^{-3}

Compound	Absorption λ_{max} / nm (ε / (L·mol^{-1}·cm^{-1})) THF				
	Soret band	Q band			
$C_3(OPTPP)_2$	427(4.45×10^5)	514(2.44×10^5)	548(1.22×10^5)	591(7.0×10^4)	648(5.4×10^4)
$Pt_2C_3(OPTPP)_2$	401(2.97×10^5)	510(2.62×10^5)	538(6.0×10^4)		
$C_4(OPTPP)_2$	410(4.38×10^5)	514(2.37×10^5)	548(1.20×10^5)	591(6.8×10^4)	648(5.1×10^4)
$Pt_2C4(OPTPP)_2$	398(2.85×10^5)	509(2.44×10^5)	539(5.1×10^4)		
$C_6(OPTPP)_2$	427(4.50×10^5)	514(2.41×10^5)	548(1.20×10^5)	591(6.6×10^4)	648(5.2×10^4)
$Pt_2C_6(OPTPP)_2$	399(2.91×10^5)	509(2.49×10^5)	538(5.9×10^4)		
$C_{10}(OPTPP)_2$	426(4.49×10^5)	513(2.39×10^5)	548(1.20×10^5)	591(6.3×10^4)	648(5.1×10^4)
$Pt_2C_{10}(OPTPP)_2$	399(2.90×10^5)	509(2.45×10^5)	538(5.2×10^4)		

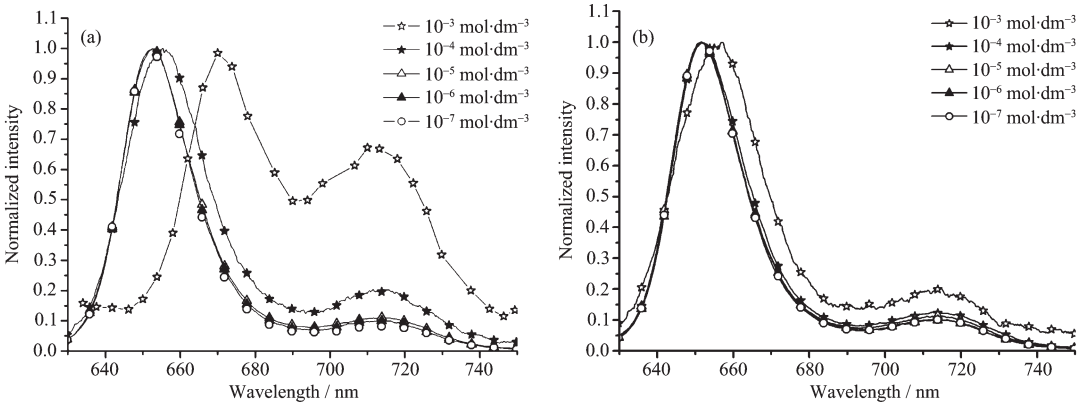

Fig.2 Normalized concentration-dependent emission spectra of (a) ligand $C_6(OPTPP)_2$ and (b) HOPTPP in THF solution at 298 K, concentration: 10^{-3}~10^{-7} mol·dm^{-3}

Table 2 Emission data of the ligands in THF solution at 298 K, concentration of 10^{-3}~10^{-7} mol·dm^{-3}

Ligand	298 K, Emission λ_{max} / nm THF									
	10^{-3} mol·dm^{-3}		10^{-4} mol·dm^{-3}		10^{-5} mol·dm^{-3}		10^{-6} mol·dm^{-3}		10^{-7} mol·dm^{-3}	
$C_3(OPTPP)_2$	668	713	655	713	652	713	652	713	652	713
$C_4(OPTPP)_2$	674	713	660	713	653	713	652	713	652	713
$C_6(OPTPP)_2$	671	713	654	713	652	713	652	713	652	713
$C_{10}(OPTPP)_2$	683	713	664	713	653	713	652	713	652	713

band at 713 nm increases obviously. The emission bands at 652 nm for C3 and C4 ligand are red-shifted to 668 and 674 nm, respectively, when ligand concentration increases from 10^{-7} to 10^{-3} mol·dm^{-3}. The emissions are more sensitive to concentration of ligand with longer aliphatic chain, and the emission maximum at 652 nm are red-shifted to 671 nm for C6 ligand and 683 nm for C10 ligand. Considering planar geometry of porphyrin molecules, it implies the existence of intermolecular or intramolecular π-π interaction. The emission spectra of mononuclear homologue (HOPTPP) in the double concentration range of diporphyrin are shown in Fig.2 (b). With concentration increases from 10^{-7} to 10^{-3} mol·dm^{-3}, the variation of the emission maxima is small in the range of 651 to 658 nm. This is a manifestation of the very weak intermolecular π-π interaction in mononuclear homologue. Therefore, it is concluded that there are intramolecular π-π interactions in diporphyrin ligands when ligand concentration increases. Ren et al[23-24] suggested that there is open or folded conformation depending on the concentration of diporphyrin molecule. Fig.3 is a schematic conformation diagram for open and folded conformation. The tendency to employ folded conformation increases with elevated concentration, and porphyrin moieties in dimer ligand get closer to each other so that the intramolecular π-π interaction can exist. When carbon atoms contained in aliphatic chain are increased, it seems easier for the ligand to form the folded conformation at high concentration. Table 3 is the data for chemical shifts of porphyrin dimers and corresponding platinum (Ⅱ) metalloporphyrin complexes. The positive shielding effects, induced by ring current both above and below porphyrin ring, result in upfield chemical shifts. When

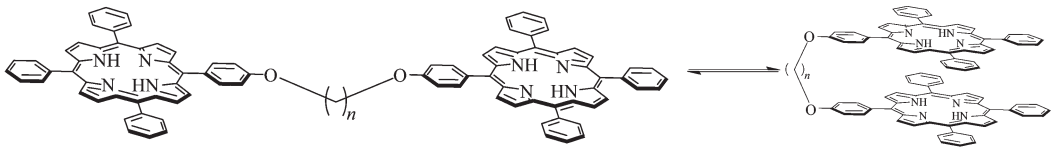

Fig.3 Schematic diagram for two different conformations of binuclear porphyrins in solution

Table 3　Chemical shifts of porphyrin dimers and corresponding platinum (Ⅱ) metalloporphyrin complexes of high (low) concentration, 10^{-3} (10^{-4}) mol·dm^{-3}

Resonance	C_3	C_4	C_6	C_{10}	C_3Pt_2	C_4Pt_2	C_6Pt_2	$C_{10}Pt_2$
β_1-pyrrolic	8.930	8.920	8.917	8.900	8.835	8.944	8.827	8.809
	(8.933)	(8.925)	(8.922)	(8.928)	(8.840)	(8.947)	(8.833)	(8.818)
β_2-pyrrolic	8.842	8.875	8.849	8.848	8.748	8.832	8.804	8.796
	(8.865)	(8.893)	(8.862)	(8.883))	(8.762)	(8.844)	(8.811)	(8.804)
β_3-pyrrolic	8.822	8.843	8.820	8.832	8.730	8.744	8.756	8.734
	(8.839)	(8.858)	(8.855)	(8.871)	(8.737)	(8.751)	(8.762)	(8.755)
o-phenyl	8.234	8.220	8.222	8.216	8.163	8.219	8.153	8.144
	(8.228)	(8.224)	(8.219)	(8.218)	(8.170)	(8.228)	(8.153)	(8.147)
o-alkoxyphenyl	8.189	8.177	8.157	8.127	8.121	8.144	8.061	8.049
	(8.176)	(8.172)	(8.144)	(8.119)	(8.117)	(8.133)	(8.053)	(8.033)
o,*p*-phenyl	7.784	7.787	7.764	7.776	7.766	7.759	7.765	7.741
	(7.982)	(7.990)	(7.958)	(7.981)	(7.778)	(7.769)	(7.778)	(7.767)
m-alkoxyphenyl	7.421	7.374	7.345	7.300	7.376	7.339	7.316	7.308
	(7.439)	(7.389)	(7.363)	(7.337)	(7.394)	(7.353)	(7.329)	(7.338)
α-CH_2	4.660	4.471	4.353	4.291	4.615	4.441	4.350	4.256
	(4.669)	(4.484)	(4.366)	(4.308)	(4.620)	(4.455)	(4.366)	(4.279)
β-CH_2	2.658	2.364	2.173	2.173	2.655	2.348	2.338	2.009
	(2.699)	(2.416)	(2.224)	(2.221)	(2.683)	(2.370)	(2.365)	(2.083)
γ-CH_2			1.857	1.725			2.104	1.551
			(1.913)	(1.799)			(2.178)	(1.621)
δ-CH_2				1.317				1.333
				(1.369)				(1.370)
ε-CH_2				0.905				0.954
				(1.002)				(1.063)
Inner NH	−2.759	−2.745	−2.769	−2.774				
	(−2.749)	(−2.737)	(−2.761)	(−2.762)				

the diporphyrin ligand is at the folded conformation on which two porphyrin rings are parallel to each other, the proton resonances would appear further at upfield. As shown in Table 3, the chemical shifts of the aliphatic methylene protons, phenyl groups on meso-sets of porphyrin ring and pyrrolic-H become smaller with increase of the length of aliphatic chain.

The normalized emission spectra data of platinum (Ⅱ) metalloporphyrin complexes in THF are shown Table 4. Because the solubility of complexes becomes poor after platinum(Ⅱ) is coordinated with porphyrin dimers, the concentration range is changed from 10^{-4} to 10^{-7} mol·dm^{-3}. As shown in Fig.4 and Table 4, similar red-shifts appear in C6, C10 complexes when concentration increases by 10^{-4} mol·dm^{-3}, while C3, C4 complexes do not show this change. This may be because of steric effect on planar rings of platinum(Ⅱ) metalloporphyrins after coordination of platinum (Ⅱ) with diporphyrin ligand, which is disadvantageous to the formation of the folded conformation of platinum(Ⅱ)

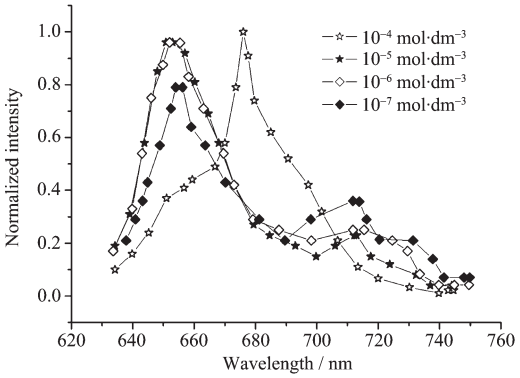

Fig.4　Normalized emission spectra of C6 complex in THF solution at 298 K, concentration of 10^{-4}~10^{-7} mol·dm^{-3}

Table 4 Emission data of the complexes in THF solution (concentration: 10^{-4}~10^{-7} mol·dm^{-3}) and in sublimate films at 298 K

Complexes	298 K, emission λ_{max} / nm THF								Sublimate films	
	10^{-4} mol·dm^{-3}		10^{-5} mol·dm^{-3}		10^{-6} mol·dm^{-3}		10^{-7} mol·dm^{-3}			
$Pt_2C_3(OPTPP)_2$	652	713	652	713	652	713	652	713	652	713
$Pt_2C_4(OPTPP)_2$	652	713	652	713	652	713	652	713	653	713
$Pt_2C_6(OPTPP)_2$	676		653	712	653	712	653	712	695	
$Pt_2C_{10}(OPTPP)_2$	681		654	712	653	712	653	712	705	

metalloporphyrin and decreases the magnitude of the π-π interaction in complexes[13]. Although steric effect reduces the π-π interaction in platinum (Ⅱ) metalloporphyrins, for longer carbon chains complexes, such as C6 and C10 complex, Pt-Pt interaction emerges with elevated concentration of platinum(Ⅱ) metalloporphyrins. Therefore, Red-shifts of emission in platinum (Ⅱ) metalloporphyrins at higher concentration should be from the π-π interaction and Pt-Pt interaction in platinum(Ⅱ) metalloporphyrins.

Fig.5 is the normalized emission spectra of the sublimate films of this series complexes. The emission spectra display more obvious red-shifts in the film than in solution, i.e. 53 nm red-shifted for C10 and 43 nm for C6 complex, while C3, C4 complexes do not show any significant changes. This indicates that the intramolecular interactions are maintained in this state as well as in solution of higher concentration. We also notice that the emission bands of C10 and C6 complexes in the sublimate film are red-shifted from 652 nm in THF solution to near-infrared region, which can make them ideal candidates for fabricating NIR elecrophosphoresent organic light-emitting devices (PhOLEDs).

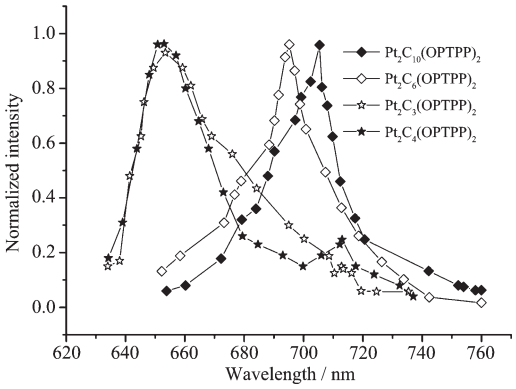

Fig.5 Normalized emission spectra of the sublimate films of platinum(Ⅱ) metalloporphyrin complexes at 298 K

2.3 Cyclic voltammetry

The electrochemical cyclic voltammetry was performed for determining the highest occupied molecular orbital (HOMO) and the lowest unoccupied molecular orbital (LUMO) of the complexes[25], which correspond to ionization potential (IP) and electron affinity (EA), respectively[25]. Fig.6 shows the cyclic voltammograms of the complexes and all related electrochemical data are summarized in Table 5. The HOMO and LUMO energy levels become lower with the increase of the length of the alkoxy chains, which indicates that the intramolecular Pt ⋯ Pt, π-π interactions improve the electron injection and transportation. Both oxidation and reduction occur primarily on Pt(Ⅱ)-porphyrin ring, so the decrease is not obvious.

2.4 Thermal properties

Fig.7 is TGA curves of the complexes. With the

Table 5 Electrochemical properties of the complexes

Complexes	λ_{edge} / nm[a]	Optical E_g / eV[b]	E_{ox}^{onset} / V vs Ag/Ag$^+$	E_{HOMO} / eV	E_{LOMO} / eV
$Pt_2C_3(OPTPP)_2$	551	2.25	1.01	−5.72	−3.55
$Pt_2C_4(OPTPP)_2$	552	2.25	1.00	−5.71	−3.57
$Pt_2C_6(OPTPP)_2$	554	2.24	1.00	−5.71	−3.61
$Pt_2C_{10}(OPTPP)_2$	559	2.22	0.99	−5.70	−3.63

[a] λ_{edge} is the onset value of absorption spectrum in long wavelength range; [b] Optical band gap is obtained from the empirical formula E_g=1 240/λ_{edge} eV.

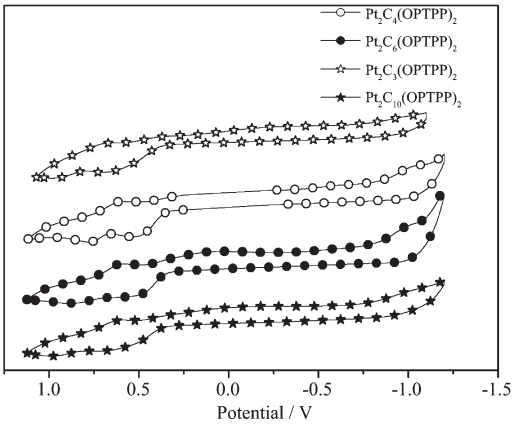

Fig.6　Cyclic voltammetry of the complexes

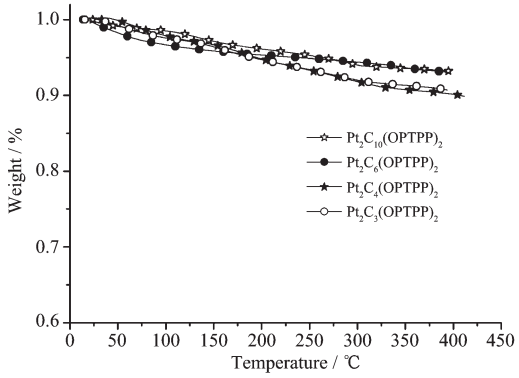

Fig.7　TGA curves of the complexes with a heating rate of 10 ℃·min^{-1} under nitrogen atmosphere

increase of the length of the chain, the thermal stability of the complexes becomes better. The temperature at 5wt% loss for C3-C10 complex is 190, 194, 238 and 263 ℃, respectively. Weight loss for all complexes is no more than 10wt% until 400 ℃.

3　Conclusions

A series of Pt (Ⅱ) dimeric metalloporphyrin complexes with aliphatic Chain of different lengths were synthesized. When the length of aliphatic chain linked the porphyrin complexes is beyond four carbon atoms, the emission spectra show obvious red-shifts in higher concentration or in sublimate film, suggesting the intramolecular π-π interactions.

References:

[1] Xiao L X, Chen Z J, Qu B, et al. *Adv. Mater.*, **2010**,**22**:1-27

[2] Brooks J, Babayan Y, Lamansky S, et al. *Inorg. Chem.*, **2002**,**41**:3055-3066

[3] Lin Y Y, Chan S C, Chan M C W, et al. *Chem. Eur. J.*, **2003**,**9**(6):1263-1272

[4] Borek C, Hanson K, Djurovich P I, et al. *Angew. Chem. Int. Ed.*, **2007**,**46**:1109-1112

[5] Borisov S M, Klimant I. *Dyes. Pigments.*, **2009**,**83**:312-316

[6] Ikai M, Ishikawa F, Aratani N, et al. *Adv. Funct. Mater.*, **2006**,**16**:515-519

[7] Luo K J, Xie Y, Xu L L, et al. *Sci. China. Chem.*, **2010**,**53**(1):167-172

[8] Williams J A G, Develay S, Rochester D L, et al. *Coord. Chem. Rev.*, **2008**,**252**:2596-2611

[9] Niedermair F, Kwon O, Zojer K, et al. *Dalton. Trans.*, **2008**, **30**:4006-4014

[10]Shavaleev N M, Adams H, Best J, et al. *Inorg. Chem.*, **2006**, **45**:9410-9415

[11]Thomas Ⅲ S W, Yagi S, Swager T M. *J. Mater. Chem.*, **2005**,**15**:2829-2835

[12]Koo C K, Lam B, Leung S K, et al. *J. Am. Chem. Soc.*, **2006**,**128**:16434-1634

[13]McGarrah J E, Kim Y J, Hissler M, et al. *Inorg. Chem.*, **2001**,**40**:4510-4511

[14]McGarrah J E, Eisenberg M. *Inorg. Chem.*, **2003**,**42**:4355-4365

[15]Ionkin A S, Marshall W J, Wang Y. *Organometallics*, **2005**, **24**:619-627

[16]Lai S W, Lam H W, Lu W, et al. *Organometallics*, **2002**,**21**: 226-234

[17]Lu W, Chan M C W, Zhu N Y, et al. *J. Am. Chem. Soc.*, **2004**,**126**:7639-7651

[18]Ma B W, Li J, Djurovich P I, et al. *J. Am. Chem. Soc.*, **2005**,**127**:28-29

[19]D′ AndraDe B, Forrest S R. *Chem. Phys.*, **2003**,**286**:321-335

[20]Cocchi M, Virgili D, Fattori V, et al. *Appl. Phys. Lett.*, **2007**,**90**(2):023506(DOI:10.1063/1.2756367)

[21]Furuta P T, Deng L, Garon S, et al. *J. Am. Chem. Soc.*, **2004**,**126**:15388-15389

[22]Deng L, Furuta P T, Garon S, et al. *Chem. Mater.*, **2006**,**18**: 386-395

[23]REN Qi-Zhi(任奇志), HUANG Jin-Wang(黄锦汪), LIN Cui-Wu(林翠梧), et al. *Chem. J. Chinese Universities.*(*Gaodeng Xuexiao Huaxue Xuebao*), **1999**,**20**(3):333-338

[24]Benthem L, Koehorst R B M, Schaafsma T J. *Maga. Reson. Chem.*, **1985**,**23**(9):732-738

[25]Yang Q, Xu Y D, Jin H, et al. *J. Polym. Sci. Part A*: *Polym. Chem.*, **2010**,**48**(7):1502-1515